PHOTONIC SENSORS / Vol. 8, No. 3, 2018: 213–219

Strong Influence of Temperature and Vacuum on the Photoluminescence of $In_{0.3}Ga_{0.7}As$ Buried and Surface Quantum Dots

Guodong WANG[1*], Huiqiang JI[2], Junling SHEN[2], Yonghao XU[1], Xiaolian LIU[1], and Ziyi FU[2]

[1]*School of Physics and Electronic Information Engineering, Henan Polytechnic University, Jiaozuo 454000, China*

[2]*School of Electrical Engineering and Automation, Henan Polytechnic University, Jiaozuo 454000, China*

*Corresponding author: Guodong WANG E-mail: wgdhpu@hotmail.com

Abstract: The strong influences of temperature and vacuum on the optical properties of $In_{0.3}Ga_{0.7}As$ surface quantum dots (SQDs) are systematically investigated by photoluminescence (PL) measurements. For comparison, optical properties of buried quantum dots (BQDs) are also measured. The line-width, peak wavelength, and lifetime of SQDs are significantly different from the BQDs with the temperature and vacuum varied. The differences in PL response when temperature varies are attributed to carrier transfer from the SQDs to the surface trap states. The obvious distinctions in PL response when vacuum varies are attributed to the SQDs intrinsic surface trap states inhibited by the water molecules. This research provides necessary information for device application of SQDs as surface-sensitivity sensors.

Keywords: Surface quantum dots; photoluminescence; temperature; vacuum; InGaAs

Citation: Guodong WANG, Huiqiang JI, Junling SHEN, Yonghao XU, Xiaolian LIU, and Ziyi FU, "Strong Influence of Temperature and Vacuum on the Photoluminescence of $In_{0.3}Ga_{0.7}As$ Buried and Surface Quantum Dots," *Photonic Sensors*, 2018, 8(3): 213–219.

1. Introduction

Quantum dots (QDs) have attracted plenty of attentions owing to their valuable properties and potential in developing the new generation of optoelectronic devices [1–3], such as solar cells [4–6], QD lasers [7, 8], semiconductor optical amplifiers [9], and light-emitting diodes [10]. As one type of quantum dots, although colloidal QDs are widely studied as fluorescent indicators and gas sensors, there are still great challenges in integrated systems and on-chip system.

In contrast, self-assembled surface QDs (SQDs) have innate advantages in integrated systems and on-chip system, due to the fact that they are grown directly on a the III-V semiconductor surface, such as GaAs and InP. In particular, the most remarkable characteristic of a sensor design based on SQDs is the fact that the extra light source and detector are not necessary. All these components can be easily made on one single III-V semiconductor materials chip. It is believed that uncapped In(Ga)As surface QDs are attractive for sensor applications like environmental monitoring of air, soil and water, food analysis, medical diagnostics, and so forth. As good examples, the sensitivity of photoluminescence

Received: 24 October 2017/ Revised: 14 March 2018

DOI: 10.1007/s13320-018-0475-z
Article type: Regular

(PL) of SQDs to polar vapor has already been demonstrated [11, 12].

But the PL from the SQDs is very weak due to the presence of non-radiative surface states. Carrier transfer related to SQDs has important influence on the improvement of PL and gas sensitivity. There is still a problem that the underlying mechanisms of coupling and carrier transfer related to SQDs is not very clear and it needs to be elaborated.

For this purpose, here, we study the photoluminescence of surface quantum dots as a function of temperature and vacuum. The carrier transfer between the surface states and SQDs confined states is analyzed by using PL and time-resolved PL (TRPL) measurements. For comparison, the buried quantum dots (BQDs) are also grown under SQDs in the hybrid QDs structure. The hybrid QDs structure is composed of one layer of $In_{0.3}Ga_{0.7}As$ SQDs and one layer of $In_{0.3}Ga_{0.7}As$ BQDs. The results show that the PL from the SQDs is significantly different from the BQDs due to the existence of the surface state.

2. Experiments

The QDs structure was grown by a solid source molecular beam epitaxy (MBE) system. As shown in Fig. 1(a), a 100-nm GaAs buffer layer was grown on an epi-ready GaAs (001) substrate at 600 ℃ following the oxide desorption at 610 ℃. Then a 21 monolayer (ML) film of $In_{0.3}Ga_{0.7}As$ was grown for the BQD layer at a substrate temperature of 505 ℃. After that, a 70-nm GaAs spacer layer and another 21 ML film of $In_{0.3}Ga_{0.7}As$ was deposited for the SQD layer. The sample temperature was immediately reduced to 350 ℃ after the SQD formation, and then the sample was unloaded from the MBE growth chamber. The formation of both SQDs and BQDs were confirmed during growth by the transition of the reflection high energy electron diffraction (RHEED) pattern from streaky to spotty.

For PL measurements, the sample was mounted into a closed-cycle cryostat (20 K–350 K) and was excited by a 200-mW diode-pumped solid state laser operated at λ=532 nm. The PL signal was measured via the standard lock-in technology with a 50-cm focal length monochrometer and an InGaAs photo-detector.

3. Results and discussion

The inserted figure of Fig. 1(b) shows an atomic force microscope (AFM) of the $In_{0.3}Ga_{0.7}As$ surface quantum dots sample. SQDs have an areal density of ~3.7×10^{10} cm^{-2}, an average height of 6.7 nm±1.3 nm, and an average diameter of 46 ± 6 nm. Defects or large incoherent islands are not found on the sample surface, indicating good QD quality.

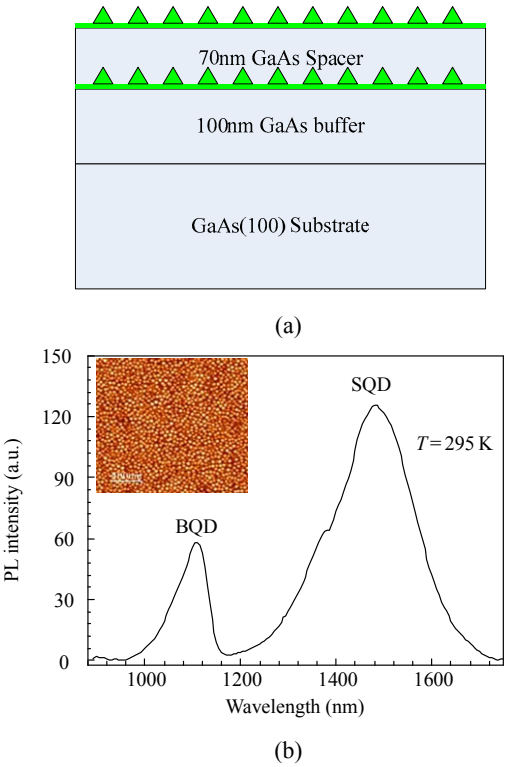

Fig. 1 Schematic of: (a) the hybrid QD structure and (b) PL spectra measured at room temperature (T=295 K) with a laser excitation intensity of 9 W/cm^2.

Room temperature (T=295 K) PL measured with a laser excitation intensity of 9 W/cm^2 is displayed in Fig. 1(b). There are two prominent PL peaks observed in the PL spectrum. The peak at ~1110 nm with a line-width [full-width-at-half-maximum, (FWHM)] of 90 nm is attributed to the emission from BQDs. The other peak at 1480 nm with an FWHM of 190 nm is attributed to the emission from SQDs. The SQDs peak shifts to the red with respect to that of BQDs by about 380 nm, because SQDs are

not strained by a capping layer and thus approach closer their natural lattice spacing and bandgap [13, 14].

In order to further study the influence of temperature on the photoluminescence spectra of BQDs and SQDs, the temperature-dependent PL measurements with the same laser excitation intensity of 9 W/cm^2 are plotted in Fig. 2. For convenience, both the BQDs and SQDs PL spectra are normalized to the maxima separately. It is noticed that the PL peaks energy shows a redshift for both BQDs and SQDs with increasing temperature due to the decreased QD bandgap predicted by the Varshni law [15, 16]. When the temperature increases from 21 K to 260 K, the redshift of the peak wavelengths of BQDs and SQDs are 60 nm and 155 nm, respectively.

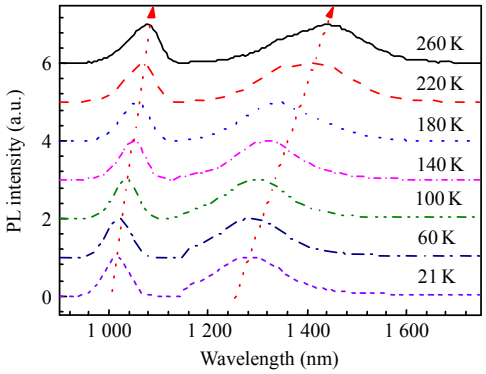

Fig. 2 PL spectra measured from 21 K to 260 K with a laser excitation intensity of 9 W/cm^2.

Figures 3(a) and 3(b) add the physical pictures by giving the FWHM as functions of temperature with the laser excitation intensity of 13 W/cm^2 and 45 W/cm^2, respectively. It can be seen that the FWHM of the BQDs and SQDs have different temperature dependences. As shown in Fig. 3(a), with the laser excitation intensity of 13 W/cm^2, the FWHM of the BQDs has a well-known behavior of narrowing as the temperature increases from 20K to 160 K. This is due to the carrier activation and redistribution to the larger (deeper) QDs via the wetting layer [17, 18]. With further increase in the temperature, FWHM of BQDs increases owing to more primary phonon scattering. It is noticed that when the laser excitation intensity increases to 45 W/cm^2, FWHM of the BQDs narrowing behavior still appears in the temperature range from 20 K to 100 K. It is obviously that the inflection point appears at low temperature when the laser excitation intensity increases from 13 W/cm^2 to 45 W/cm^2. It can be illustrated as follows. When the laser excitation intensity increasing the quantity of photo-induced carriers is sufficient, the process of carrier redistribution accomplishes ahead at a low temperature. Conversely, according to [19], there are no confined electron states in the surface wetting layer, which is along with surface trap states and prevents the large scale redistribution of carriers between SQDs. Thus, we expect the line width of SQDs behaves differently with the BQDs with increasing temperature. As shown in Fig. 3(b), FWHM of the SQDs increases monotonically as the temperature increases.

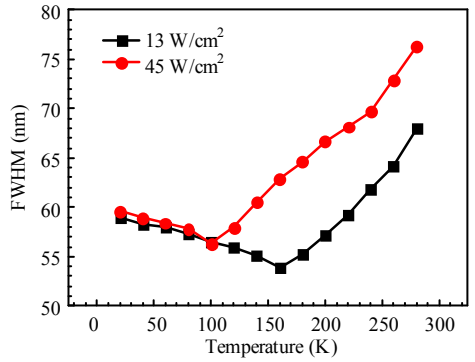

(a)

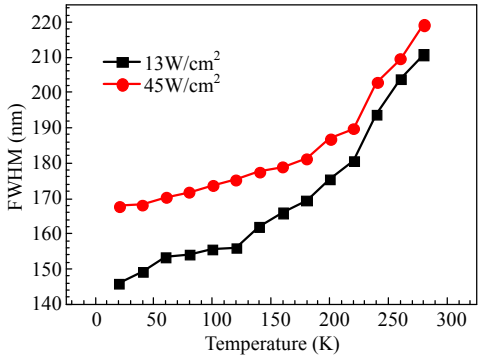

(b)

Fig. 3 FWHM of the PL peaks from (a) BQDs and (b) SQDs as functions of temperature.

The PL spectra at 77 K by using different laser wavelengths but the same laser excitation intensity

are also investigated. As shown in Fig. 4(a), each spectrum is normalized to the maximum intensity of the BQD peak. The ratio of the integrated PL intensity (R = SQDs/BQDs) as a function of the excitation laser wavelength is displayed in Fig. 4(b). It is observed that the PL spectral profiles and PL intensity ratio change by using different excitation wavelengths. When the excitation photon energy reaches the GaAs bandgap (820 nm), the SQDs emission gets the minimum intensity. This excitation wavelength dependence enriches our understanding of the carrier dynamics inside the studied QD structure. We believe that for a laser with photon energy above GaAs bandgap, the photon-excited carriers are predominantly generated in the GaAs buffer spacer layers and then relax into the ground-state energy levels of the BQDs and SQDs. For the BQDs, once the excitation photon energy matches with the GaAs bandgap energy, i.e., resonant excitation happens, the BQDs will endure an enhancement for carrier generation in the GaAs layers. Consequently, carrier collection and combination enhancement happen inside BQDs. However, for the carriers collected by the SQDs, no matter whether they are generated in the GaAs matrix, in the wetting layers, or in the QD initially, most of them will go to surface states due to the strong coupling between the confined quantum states in SQDs and the surface states. Therefore, the laser wavelength variation has less effect on the SQD PL emission intensity. As a result, we observe a relatively minimum value for the SQD PL intensity in Fig. 4(a) as well as a minimum value for the integrated PL intensity ratio in Fig. 4(b) at a laser wavelength of 820 nm.

The PLs of the BQDs and SQDs are also measured under different vacuums at room temperature as recorded in Fig. 5. A molecular pump and vacuometer are used to pump out and monitor vacuum. As shown in Fig. 5, when the vacuum of the test chamber increases, a remarkably decrease in the SQDs PL intensity is observed without changes in the emission position and band shape. The peak wavelength of SQDs PL is fixed at 1460 nm, and the FWHM is about 190 nm when the vacuum varies from 12 mbar to 0.003 mbar. However, when the pressure increases to 12 mbar, the integrated PL intensity of SQDs increases to 2 times of that as the pressure is 0.0003 mbar. This enormous change about integrated PL intensity of SQDs can be attributed to an increase in water molecules in the test chamber with the vacuum increasing. As we know, water molecules are polar. So it can be adsorbed on the surface of SQDs, and the SQDs intrinsic surface trap states can be inhibited by the water molecules. Water molecules being adsorbed on the surface of SQDs have the ability to donate electron density to the surface states, saturating a certain number of these non-radiative sites. In turn, more electrons become available for the radiative recombination, which results in an increase in the overall PL intensity. The enhancements of SQDs PL

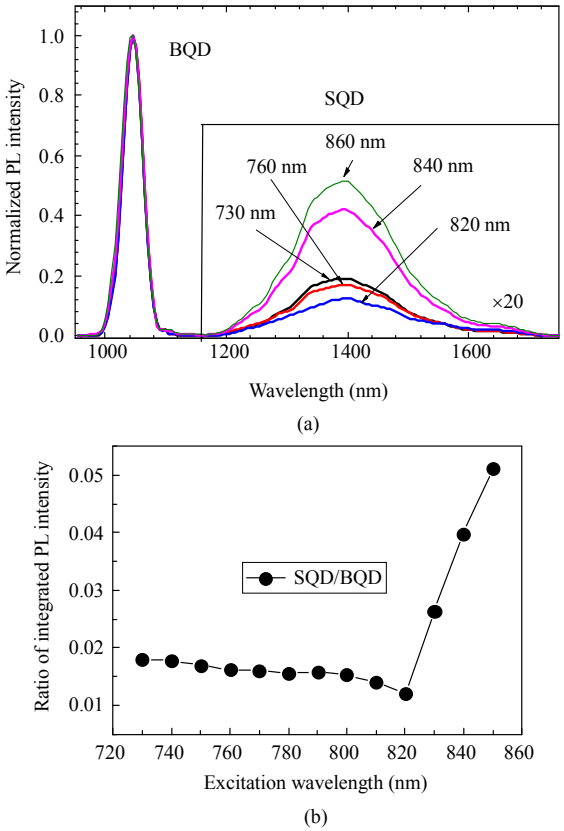

Fig. 4 PL spectra of BQDs and SQDs with different excitation laser wavelengths: (a) PL spectra at 77K and (b) integrated PL intensity ratio of SQDs to BQDs as a function of different excitation laser wavelengths.

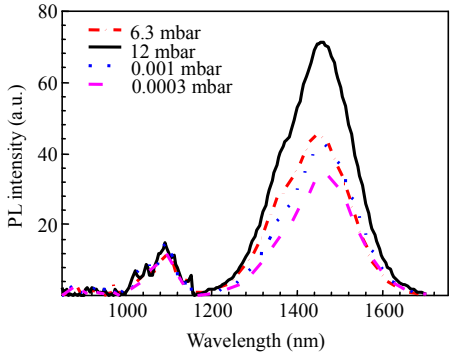

Fig. 5 PL spectra of BQDs and SQDs with different vacuums.

intensity by the polar molecules have also been reported by other research groups [20–22]. Conversely, there are no obvious varieties in the BQDs PL spectra as the vacuum decreases, as shown in Fig. 5. The reason is that the surface states have almost no effect on BQDs because of the existence of capped layer on the BQDs.

The TRPLs of the SQDs and BQDs are also measured under different vacuums. For these measurements, the excitation is switched to a super-continuum laser operated at 532 nm, and the PL is detected by a time-correlated single photon counting system with a fast photomultiplier tube detector. Figures 6(a) and 6(b) show the TRPL spectra measured at 12 mbar and 0.0003 mbar, respectively. For BQDs, the vacuum has almost no effect on the TRPL. It exhibits a mono-exponential decay with a time constant (carrier lifetime). This agrees well with most reported lifetimes of InGaAs QDs. However, SQDs exhibit a different decay behavior when the test chamber vacuum varies. With the vacuum increasing from 12 mbar to 0.0003 mbar, the lifetime of SQDs becomes longer. The reason is that the quantity of inhibited surface trap states is weakened due to a decrease in water molecules. It means that more electrons transfer from surface QD confined states to the surface trap states, and the non-radiative recombination is enhanced. In turn, fewer electrons become available for the radiative recombination, which results in a longer lifetime of SQDs.

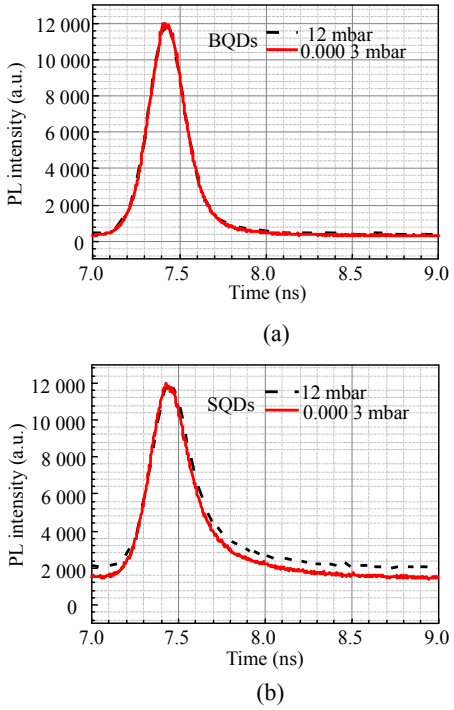

Fig. 6 TRPL of: (a) BQDs and (b) SQDs with different vacuums.

4. Conclusions

In summary, the optical properties of $In_{0.3}Ga_{0.7}As$ SQDs and BQDs are comparatively studied by PL and TRPL measurements when the temperature and vacuum vary. The results indicate that the optical performance of the SQDs is significantly different from the BQDs. The main differences in PL response, both steady state and transient, are attributed to carrier transfer from SQDs to the surface trap states. The obvious distinctions in PL response when vacuum varies are attributed to the SQDs intrinsic surface trap states inhibited by the water molecules. This research has enriched the physical picture of photo-excited carriers inside SQDs and it provides necessary information for device applications of SQDs as surface-sensitivity sensors.

Acknowledgment

The authors gratefully acknowledge the supports from the National Natural Science Foundation of China (Grant No. U1304608), the Project of Henan

Provincial Department of Science and Technology (Grant No. 182102410047), and the Program of Henan Polytechnic University (Grant No. T2015-3).

References

[1] A. W. Walker, S. Hechelmann, C. Karcher, O. Hohn, C. Went, M. Niemeyer, *et al.*, "Nonradiative lifetime extraction using power-dependent relative photoluminescence of III-V semiconductor double-heterostructures," *Journal of Applied Physics*, 2016, 119(15): 155702-1–155702-10.

[2] H. Saito, K. Nishi, and S. Sugou, "Influence of GaAs capping on the optical properties of InGaAs/GaAs surface quantum dots with 1.5 μm emission," *Applied Physics Letters*, 1998, 73(19): 2742–2744.

[3] G. D. Wang, B. L. Liang, B. C. Juang, A. Das, M. C. Debnath, D. L. Huffaker, *et al.*, "Comparative study of photoluminescence from $In_{0.3}Ga_{0.7}As$/GaAs surface and buried quantum dots," *Nanotechnology*, 2016, 27(46): 465701-1–465701-6.

[4] D. Chettri, T. J. Singh, and K. J. Singh, "InAs/GaAs quantum dot solar cell," *International Journal of Electronics, Electrical and Computational System*, 2017, 6(3): 221–224.

[5] A. D. Utrilla, D. F. Reyes, J. M. Llorens, I. Artacho, T. Ben, D. Gonzalez, *et al.*, "Thin GaAsSb capping layers for improved performance of InAs/GaAs quantum dot solar cells," *Solar Energy Materials & Solar Cells*, 2017, 159: 282–289.

[6] K. Sablon, J. Little, N. Vagidov, Y. Li, V. Mitin, and A. Sergeev, "Conversion of above- and below bandgap photons via InAs quantum dot media embedded into GaAs solar cell," *Applied Physics Letters*, 2014, 104(25): 253904-1–253904-5.

[7] B. Shi, S. Zhu, Q. Li, Y. T. Wan, E. L. Hu, and K. M. Lau, "Continuous-wave optically pumped 1.55 um InAs/InAlGaAs quantum dot microdisk lasers epitaxially grown on silicon," *ACS Photonics*, 2017, 4: 204–210.

[8] F. Gao, S. Luo, H. M. Ji, X. G. Yang, and T. Yang, "Enhanced performance of tunable external-cavity 1.5 μm InAs/InP quantum dots lasers using facet coating," *Applied Optics*, 2015, 54(3): 472–476.

[9] A. Zeghuzi, H. Schmeckebier, M. Stubenrauch, C. Meuer, C. Schubert, C. A. Bunge, *et al.*, "25 Gbits differential phase-shift-keying signal generation using directly modulated quantum dot semiconductor optical amplifiers," *Applied Physics Letters*, 2015, 106: 213501-1–213501-4.

[10] S. M. Chen, W. Li, Z. Y. Zhang, D. Childs, K. J. Zhou, J. Orchard, *et al.*, "GaAs-based superluminescent light emitting diodes with 290 nm emission bandwidth by using hybrid quantum well/quantum dot structures," *Nanoscale Research Letters*, 2015, 10(1): 1–8.

[11] R. D. Angelis, M. Casalboni, F. D. Matteis, F. Hatami, W. T. Masselink, H. Zhang, *et al.*, "Chemical sensitivity of InP/$In_{0.48}Ga_{0.52}P$ surface quantum dots studied by time-resolved photoluminescence spectroscopy," *Journal of Luminescence*, 2015, 168: 54–58.

[12] M. J. Milla, J. M. Ulloa, and A. Guzman, "Strong Influence of the humidity on the electrical properties of InGaAs surface quantum dots," *ACS Applied Materials & Interfaces*, 2014, 6(9): 6191–6195.

[13] R. D. Angelis, L. D. Amico, M. Casalboni, F. Hatami, W. T. Masselink, and P. Prosposito, "Photoluminescence sensitivity to methanol vapours of surface InP quantum dots: effect of dot size and coverage," *Sensors & Actuators B: Chemical*, 2013, 189(2): 113–117.

[14] B. L. Liang, Z. M. Wang, Y. I. Mazur, S. Seydmohamadi, M. E. Ware, and G. J. Salamo, "Tuning the optical performance of surface quantum dots in InGaAs/GaAs hybrid structures," *Optics Express*, 2007, 15(3): 8157–8162.

[15] Z. X. Zhao, R. B. Laghumavarapu, P. J. Simmonds, H. M. Ji, B. A. Liang, and D. L. Huffaker, "Photoluminescence study of the effect of strain compensation on InAs/AlAsSb quantum dots," *Journal of Crystal Growth*, 2015, 425: 321–315.

[16] I. Vurgaftman, J. R. Meyer, and L. R. Ram-Mohan, "Band parameters for III-V compound semiconductors and their alloys," *Journal of Applied Physics*, 2001, 89(11): 5815–5875.

[17] D. I. Lubyshev, P. P. Gonzalez-Borrero, E. Marega, E. Petitprez, N. L. Scala, and P. Basmaji, "Exciton localization and temperature stability in self-organized InAs quantum dots," *Applied Physics Letters*, 1996, 68(2): 205–207.

[18] Z. Y. Xu, Z. D. Lu, Z. L. Yuan, X. P. Yang, B. Z. Zheng, J. Z. Xu, *et al.*, "Thermal activation and thermal transfer of localized excitons in InAs self-organized quantum dots," *Superlattices and Microstructures*, 1998, 23(2): 381–387.

[19] J. Z. Wang, Z. Yang, and C. L. Yang, "Photoluminescence of InAs quantum dots grown on GaAs surface," *Applied Physics Letters*, 2000, 77(18): 2837–2839.
[20] M. J. Milla, J. M. Ulloa, and A. Guzman, "Strong influence of the humidity on the electrical properties of InGaAs surface quantum dots," *ACS Applied Materials & Interfaces*, 2014, 6(9): 6191–6195.
[21] M. J. Milla, J. M. Ulloa, and A. Guzman, "Photoexcited induced sensitivity of InGaAs surface QDs to environment," *Nanotechnology*, 2014, 25(44): 445501-1–445501-6.
[22] R. D. Angelis, M. Casalboni, F. D. Matteis, F. Hatami, W. T. Masselink, H. Zhang, *et al.*, "Chemical sensitivity of InP/$In_{0.48}Ga_{0.52}$P surface quantum dots studied by time-resolved photoluminescence spectroscopy," *Journal of Luminescence*, 2015, 168: 54–58.